Porras, MA.; Ramos Pascual, F. (2017). Quasi-ideal dynamics of vortex solitons embedded in flattop nonlinear Bessel beams. OPTICS LETTERS. 42(17):3275-3278. doi:10.1364/OL.42.003275

Quasi-ideal dynamics of vortex solitons embedded in flat-top nonlinear Bessel beams

MIGUEL A. PORRAS[1,*] AND FRANCISCO RAMOS[2]

[1]Grupo de Sistemas Complejos, ETSIME, Universidad Politécnica de Madrid, Rios Rosas 21, 28003 Madrid, Spain
[2]Nanophotonics Technology Center, Universitat Politècnica de València, Camino de Vera s/n, 46022 Valencia, Spain
[*]Corresponding author: miguelangel.porras@upm.es

Compiled July 17, 2017

The applications of vortex solitons are severely limited by the diffraction and self-defocusing spreading of the background beam where they are nested. Nonlinear Bessel beams in self-defocusing media are non-diffracting, flat-top beams where the nested vortex solitons can survive for propagation distances that are one order of magnitude larger than in the Gaussian or super-Gaussian beams. The dynamics of the vortex solitons is studied numerically and is found to approach that in the ideal, uniform background, preventing vortex spiraling and decay, which eases vortex steering for applications.

OCIS codes: *(050.4865) Optical vortices; (190.0190) Nonlinear optics*

http://dx.doi.org/10.1364/ao.XX.XXXXXX

An optical vortex soliton (OVS) is an intensity dip carrying a phase dislocation in a bright background field [1–3]. Even if the balance between diffraction and self-defocusing nonlinearity is stable in a single OVS, its propagation as such is always limited by the finiteness of the background beam where the OVS has to be inserted in any real setting. Self-defocusing accelerates diffraction of the finite background [3, 4], which severely limits the applications of OVSs and OVS arrays as, e. g., waveguides for other beams, particle and atom trapping [3, 5–7], soliton stabilization [8], and enhanced second harmonic generation [9]. Also, inhomogeneity of the intensity and phase of the background, typically a broad Gaussian or super-Gaussian (SG) beam, complicates the OVS dynamics and interactions of OVSs in arrays, which led to an intense study of OVS dynamics with the aim of steering their motion [10–14]. These problems probably led to consideration of other configurations, such as ring-shaped (localized) OVSs [2] in media with self-focusing or more complex self-defocusing nonlinearities [15, 16], which can also guide other waves [17], but are limited to the single vortex of the ring soliton, excluding applications such as reconfigurable arrays of OVS-induced waveguides.

Surprisingly, embedding one or many OVSs in a nondiffracting beam in the self-defocusing medium has not been considered before, to our knowledge. These beams indeed exist, and their finite-power versions are generated experimentally, in the form of fundamental nonlinear Bessel beams (NBBs) [18], and high-order NBBs, not described previously in self-defocusing media, since most of research focused on positive Kerr nonlinearity [19–23]. As shown here, these beams may present arbitrarily wide regions of uniform intensity and phase that propagate without any change for long distances, only limited by instability effects. We show that NBBs with wide plateau can be generated placing a standard Bessel beam generator in front of the nonlinear medium. We then consider OVSs nested in the plateau of fundamental NBBs to show that they survive as OVSs and interact closely approaching the much simpler dynamics in the uniform background, for distances that are one order of magnitude larger than in standard backgrounds of similar size. E. g., a single off-axis OVS can remain undistorted and at rest, and an OVS pair rotate uniformly more than 360° in a circular orbit, in about 70 nonlineal lengths, approximately ten times the distances and angles reported in [14], and four times the angles in [12]. Our analysis also offers a unified view of the nature of the OVS-background system as a particular vortex-carrying conical beam in the self-defocusing medium, offering new possibilities for their generation.

As is well-known, OVSs are solutions of the form $A = \sqrt{I_0}\, b(r) e^{im\varphi} e^{i\delta z}$ to the nonlinear Schrödinger equation (NLSE)

$$\partial_z A = \frac{i}{2k}\Delta_\perp A + i\frac{kn_2}{n}|A|^2 A\,, \tag{1}$$

describing monochromatic light beam propagation in a medium with $n_2 < 0$ [2] in the paraxial approximation to the Helmholtz wave equation. In the above equations, (r, φ, z) are cylindrical coordinates, $\Delta_\perp = \partial_r^2 + (1/r)\partial_r + (1/r^2)\partial_\varphi^2$ is the transversal Laplacian operator, A is the complex envelope of the monochromatic light beam $E = A\exp[-i(\omega t - kz)]$ of angular frequency ω and propagation constant $k = (\omega/c)n$ in a medium of linear refractive index n. The axial wavenumber of OVSs is shortened by $\delta < 0$, related to its background intensity by $I_0 = n|\delta|/k|n_2|$, and the radial profile verifies $b(r) \to 1$ as $r \to \infty$ and $b(r) \sim r^{|m|}$ as $r \to 0$, where the vortex of topological charge $m = \pm 1, \pm 2, \ldots$ is located.

We find it convenient to study OVSs and their dynamics using the dimensionless coordinates and envelope $\zeta = |\delta|z, \rho =$

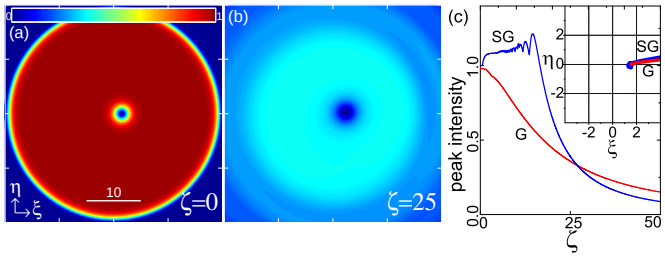

Fig. 1. (a,b) A singly-charged vortex ($m = 1$) initially displaced 1.5 from the center of the SG background $u_{BG} = \exp[-(\rho/19.7)^{40}]$ at the indicated distances. As indicated, the distance between axis ticks is 10. (c) Peak intensity versus propagation distance for the above SG-vortex system, and for the Gaussian beam $u_{BG} = \exp[-(\rho/32.6)^2]$ of the same FWHM = 38.4 and with the same nested vortex. Inset in (c): trajectory of the vortices in both cases.

$\sqrt{k|\delta|}r$ and $u = \sqrt{k|n_2|/n|\delta|}A$. For comparison purposes, the characteristic nonlinear length $L_{\rm NL} = 1/k|n_2|I_0$ corresponds to $\zeta_{\rm NL} = 1$. The dimensionless NLSE is

$$\partial_\zeta u = \frac{i}{2}\Delta_\perp u - i|u|^2 u\,, \qquad (2)$$

where now $\Delta_\perp = \partial_\rho^2 + (1/\rho)\partial_\rho + (1/\rho^2)\partial_\varphi^2$, and the OVS is $u_m = b_m(\rho)e^{im\varphi}e^{-i\zeta}$, where the exact radial profile $b_m(\rho)$ of the OVS is determined by

$$\frac{d^2b}{d\rho^2} + \frac{1}{\rho}\frac{db}{d\rho} - \frac{m^2}{\rho^2}b + 2b - 2b^3 = 0\,, \qquad (3)$$

subjected to the boundary conditions $b_m(\rho) = C_{|m|}\rho^{|m|}$ as $\rho \to 0$ and $b_m(\rho) \to 1$ as $\rho \to \infty$. These conditions are satisfied for the specific values $C_1 \simeq 0.824754$, $C_2 \simeq 0.306198$,.... The corresponding radial profiles can be approached by $b_m(\rho) \simeq [\tanh(C_{|m|}^{1/|m|}\rho)]^{|m|}$. In Ref.[13], $b_1(\rho) \simeq \tanh(0.787\rho)$ is used because it gives a better overall fitting (not only at $\rho \to 0$). For more details, see, e. g., [2].

According to the above, an unlimited background surrounds the OVS. In practice, OVSs are usually nested in a broad Gaussian beam, or in a flatter SG beam [4, 11, 14], where they undergo a complex individual or interaction dynamics governed by their topological charges, mutual disposition, and the phase and intensity gradients of the background [10–14]. In either case, OVSs are eventually dispersed when joint action of diffraction and self-defocusing expand the background. In our examples of OVS dynamics, the initial condition in the NLSE (2) is of the type $u(\xi,\eta,\zeta = 0) = u_{\rm BG}\prod_{j=1}^{N} u_{m_j}(\xi,\eta)$. In this expression, $(\xi,\eta) = \sqrt{k|\delta|}(x,y)$ are dimensionless Cartesian coordinates, $u_{m_j}(\xi,\eta) = b_{m_j}(\rho_j)e^{im_j\varphi_j}$ are N OVSs of charges m_j placed at the points (ξ_j,η_j) of the background field $u_{\rm BG}$, and (ρ_j,φ_j) are polar coordinates with origin at (ξ_j,η_j), i. e., $\rho_j = [(\xi-\xi_j)^2 + (\eta-\eta_j)^2]^{1/2}$, $\varphi = \tan^{-1}[(\eta-\eta_j)/(\xi-\xi_j)]$. The radial profile of each OVS is obtained by solving numerically (3) with the indicated boundary conditions, but in practice their approximations in terms of tanh functions can be used as well. The NLSE (2) with the initial condition $u(\xi,\eta,\zeta = 0)$ is then solved numerically using a grid in (ξ,η).

For example, the single vortex slightly displaced from the Gaussian or SG center in Fig. 1 widens as the background intensity diminishes [Figs. 1(a,b)] and moves almost radially outwards [inset of Fig. 1(c)]. In contrast, the single vortex would subsist forever as an OVS at rest in the infinite background. Fig. 2 illustrates the interaction dynamics of two equal vortices in uniform, Gaussian and SG backgrounds. The two vortices broaden and spiral-out as the background intensity diminishes, while the vortices in the ideal background simply rotate indefinitely at constant angular velocity following circular trajectories [aside the initial transient of reshaping from $b_1(\rho) \simeq \tanh(0.787)$ to the exact 2-OVS structure seen in Fig. 2(h)]. In these examples, the FWHMs of the backgrounds compared to the vortex sizes are similar to those in Refs. [13, 14].

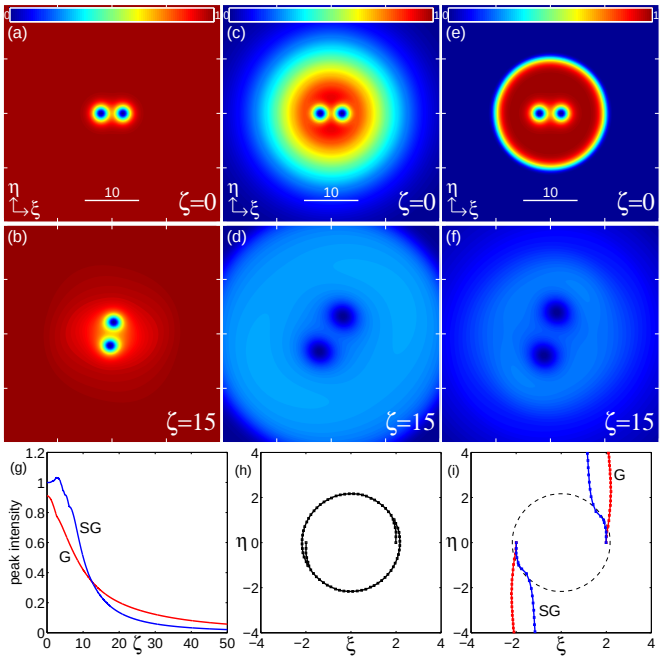

Fig. 2. Two singly-charged vortices separated $d = 4$ in (a,b) uniform (c,d) Gaussian $u_{BG} = \exp[-(\rho/16.6)^2]$ and (e,f) SG $u_{\rm BG} = \exp[-(\rho/10.7)^{15}]$ backgrounds, at the indicated distances. As indicated, the distance between ticks is 10. (g) Peak intensity versus propagation distance for the Gaussian-vortex and SG-vortex systems. Vortex trajectories in (h) the uniform background and in (i) the Gaussian and SG backgrounds.

We consider nesting OVSs in the propagation-invariant NBBs supported by the self-defocusing medium. Unlike the Kerr-compressed, highly unstable NBBs in transparent media with $n_2 > 0$ [18, 24], NBBs with $n_2 < 0$ may have arbitrarily wide and flat, intensity profiles and their instability is weaker. In addition, there is an close connection between these NBBs and OVSs. NBBs are solutions to (1) of the same form as OVSs, i. e., $A = \sqrt{I_0}\,b(r)e^{im\varphi}e^{i\delta z}$, with $\delta < 0$ too, but $b(r)$ approaches zero at large radius as $b_\infty J_m(k\theta r)$, where $\theta = \sqrt{2|\delta|/k}$ is the cone angle, and b_∞ is a constant. Therefore $I_0 = n|\delta|/k|n_2|$ has not the meaning of a background intensity for NBBs. In our dimensionless variables, NBBs read $u = b(\rho)e^{im\varphi}e^{-i\zeta}$, with $b(\rho)$ satisfying also (3) with the boundary condition $b(\rho) = C\rho^{|m|}$ as $\rho \to 0$, but approaching zero as $b_\infty J_m(\sqrt{2}\rho)$. As for OVSs, no analytical solution can be found, but solutions are numerically seen to exist for $0 < C < C_0 \equiv 1$ for $m = 0$, and for

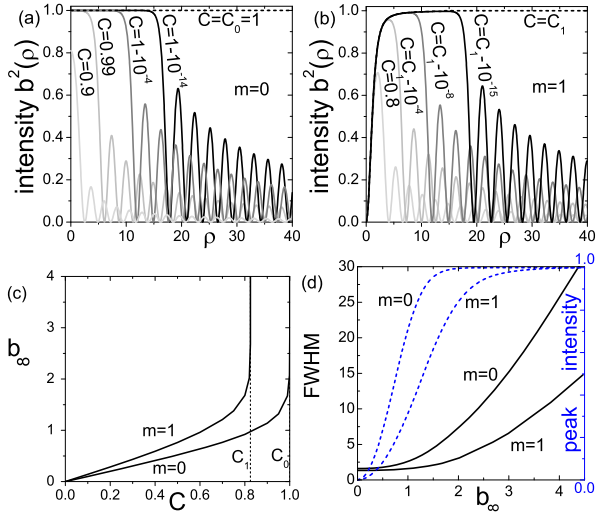

Fig. 3. (a,b) Radial intensity profiles of NBBs with increasing C featuring increasingly wide region of flat unit intensity. The limit $C \to C_{|m|}$ is the uniform nonlinear plane wave (for $m = 0$) and the OVS (for $|m| > 0$), shown as dashed curves. (c) Amplitude b_∞ of the linear Bessel tail as a function of C. (d) FWHM of the central maximum or inner ring (solid curves) and its intensity (dashed curves) as functions of b_∞.

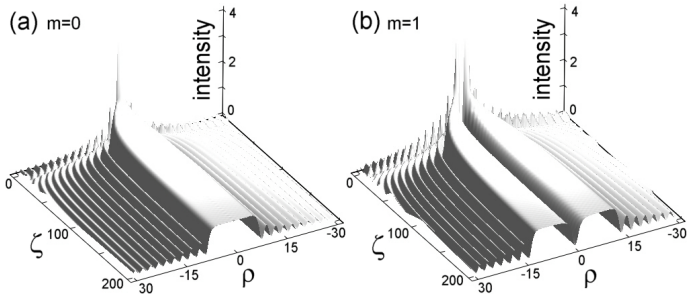

Fig. 4. Propagation of input Bessel beams $b_\infty J_m(\sqrt{2}\rho)e^{im\varphi}$ in a self-defocusing medium. In (a), $m = 0$, $b_\infty = 3.2$. The formed NBB has unit peak amplitude and FWHM of about 15, as predicted by Fig. 3(d). In (b), $m = 1$, $b_\infty = 4.1$. The formed NBB has unit peak amplitude and FWHM of the first ring of about 12.5, as predicted by Fig. 3(d).

$0 < C < C_{|m|}$ for each given charge of the vortex $\rho = 0$.

The limit of low C is the linear Bessel beam. As C increases, the intensity profile features wider and flatter central maximum of dimensionless intensity very close to unity (intensity I_0) for the fundamental NBB ($m = 0$), and wider and flatter inner ring of intensity also close to unity for high-order NBBs ($|m| > 0$) [Figs. 3(a) and (b)]. The uniform nonlinear plane wave $b(\rho) = 1$ for $m = 0$, and the OVS of the corresponding charge $m \neq 0$ correspond to the limits $C \to C_{|m|}$ [dashed curves in Figs. 3(a) and (b)]. Thus, for NBBs, I_0 is the maximum attainable intensity, given a cone angle. The OVS of topological charge $m \neq 0$ is the limiting NBB of the same charge as the inner ring becomes infinetely wide. Vice versa, the NBB with $m \neq 0$ and wide inner ring can be considered as the natural, finite background where the vortex in its center can subsist for long distances, only limited by the instability effects considered below.

The amplitude b_∞ of the linear Bessel tails, $b_\infty J_m(\sqrt{2}\rho)$, as obtained from the NBB numerical profiles, [Fig. 3(c)] grows monotonously from 0 up to ∞ with C increasing from 0 to $C_{|m|}$. As seen below, b_∞ is a directly accessible parameter in the proposed experimental generation of NBBs. It is then more practical to specify a NBB by b_∞, ranging from 0 to ∞, than by C. Figure 3(d) shows that the FWHM of the central maximum of intensity (for $m = 0$), or of the inner ring (for $m = 1$), and the peak intensity, grows without bound and stabilizes in unity, respectively, as b_∞ increases (C approaches $C_{|m|}$).

Figure 4 illustrates how NBBs with wide plateau can be generated. Both in Fig. 4(a) for $m = 0$ and (b) for $m = 1$ the initial condition in the NLSE (2) is the linear Bessel beam $b_\infty J_m(\sqrt{2}\rho)e^{im\varphi}$ of the amplitude b_∞. Extrapolating the results in Ref. [21] for self-focusing media to self-defocusing media, the NBB that is spontaneously formed from the input linear Bessel beam at long enough propagation distances is that preserving the amplitude of the linear Bessel tail, b_∞. Therefore, the width of the plateau of the NBB can be predicted from the amplitude b_∞ of the input linear Bessel beam and Fig. 3(d). According also to Fig. 3(d), the higher the intensity of the input linear Bessel beam, the wider the plateau of the formed NBB.

Our simulations show that OVSs embedded in flat NBBs survive for much longer distances than in Gaussian or SG backgrounds, and that the vortex dynamics is particularly simple, approaching that in the infinite background. Also, nesting the OVS in the NBB plateau does not appreciably destabilize it, but instability initiates in the NBB periphery, allowing the quasi-ideal OVS dynamics to continue even if the background initiates to disintegrate. For example, the only difference in Fig. 5 with respect to Fig. 1 is that the background is a vortex-less NBB of the same FWHM and similar flatness as the SG background. The NBB-OVS system propagates without appreciable change up to $\zeta \sim 55$, while distortions were already present at $\zeta \sim 5$ with the SG background. At $\zeta = 55$ the instability of the NBB starts to develop. A linear-instability analysis, as those reported in Refs. [2, 24], reveals that vortex-less NBBs are unstable above a certain value of C, i. e., above a certain width of the central maximum. Also, the so-called winding number [2] of the dominant unstable mode (number of fragments in the azimuthal direction in which the NBB will break) are increasingly high (e. g., 20 for the most unstable mode of the NBB in Fig. 5). Unstable modes of such a high winding number are highly delocalized and are not easily excited by perturbations inside the flat central maximum, e.g., by the nested OVS. Indeed instability is first observed in the periphery of the plateau region and first rings, endowing the periphery with a polygonal shape with a number of sides equal to the winding number of the dominant mode, but leaving its interior and the OVS substantially unaltered, as seen in Fig. 5(b). Additional simulations confirm that instability onsets at approximately the same distance with or without embedded vortex. As seen in Fig. 5(c) for the regime of well-developed instability, the OVS still survives at rest. Of course, the ulterior development of instability leads to the destruction of the NBB-OVS system.

Similarly, the only difference in Fig. 6(a-c) with respect to Fig. 2(c-f) is the NBB background, which however has the same FWHM. Instability of the NBB is weaker because of its narrower plateau, but the two OVS are closer to its boundary. All together, the whole system propagates without appreciable distortion up to a similar distance $\zeta \sim 55$ as in the preceding

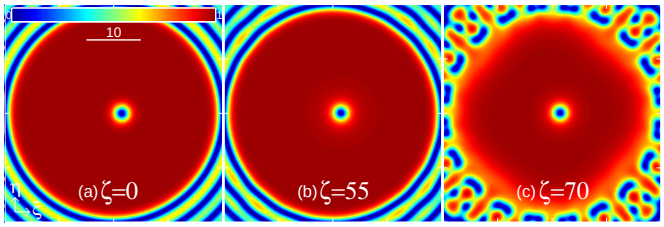

Fig. 5. A singly-charged OVS initially displaced 1.5 from the center of the NBB background with $b_\infty = 4.93$, having a central maximum of FWHM = 38.4, as the backgrounds in Fig. 1, at the indicated propagation distances.

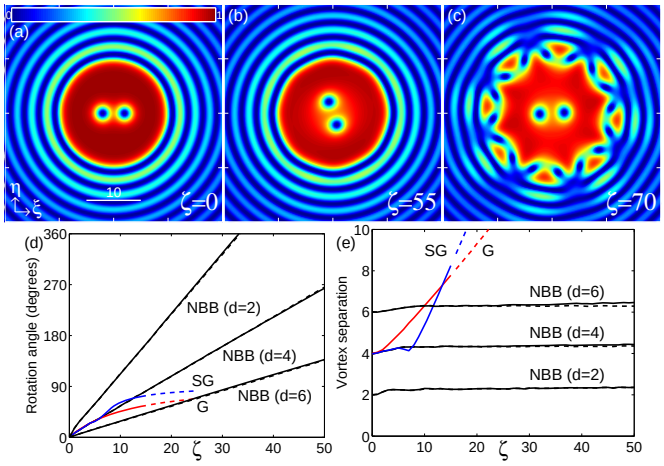

Fig. 6. (a-c) Two singly-charged OVSs initially separated $d = 4$ in the fundamental NBB background with $C = 1 - 10^{-8}$, or $b_\infty = 3.45$, and FWHM $\simeq 20$, at the indicated propagation distances. (d) Rotation angle and (e) separation distance of the two OVSs as functions of propagation distance, for separations $d = 2, 4$ and 6 (solid curves), compared to the same quantities in the uniform background (dashed curves). The G and SG curves are for Gaussian and SG backgrounds with $d = 4$.

example, where instability arises as a weak octagonal distortion, and leads to complete destruction beyond $\zeta = 70$. Importantly, the two OVSs are seen in Figs. 6(a-c) to rotate at uniform angular velocity at a constant separation up to that distance, as in the ideal uniform background in Figs. 2(a-b), while in the non-uniform backgrounds of Figs. 2 (c-f), broadening, spiraling and deceleration are already significant at $\zeta \sim 10$ [14]. This is further supported by Figs. 6(d) and (e), where the dynamics of the two OVSs (rotation angle and OVS separation) placed initially at different distances ($d = 2, 4$ and 6) in the NBB and in the uniform background are seen to be almost identical, and therefore are not subjected to the inhomogeneities and spreading effects that complicates the vortex dynamics. In contrast to previous simulations and experiments, in which the maximum reported rotation is about 180° (including significant broadening and spiraling), rotations larger than 360° without deformation or distancing are easily attainable, as in Fig. 6(c) for $d = 4$ at $\zeta = 70$ or for $d = 2$ at $\zeta = 33$ in Fig. 6(d).

In summary, we have reported the properties of fundamental and high-order NBBs in self-defocusing media. OVSs nested in the fundamental NBB can survive unaltered for distances that are one order of magnitude larger than in wide Gaussian or SG backgrounds, featuring a particularly simple and predictable dynamics and interactions. This is a natural consequence of two properties of NBBs: they do not diffract and may have a wide region of constant intensity and phase, so that the OVSs actually "feel" an almost uniform background transversally and longitudinally that mimics the ideal plane wave. Also, the OVSs do not appreciably destabilize the hosting NBB. These results will hold substantially unaltered with laboratory-generated, finite-power NBBs as long as their diffraction-free distance is larger than that of the instability development. Further research is necessary to lower or suppress the instability initiating in the plateau periphery, thus lengthening the quasi-ideal propagation distance of the OVSs. These results open new perspectives in applications such as optical vortex-induced waveguides, particle trapping and laser material processing, where precise steering of the OVSs is a crucial issue.

Funding. National Science Foundation (NSF) (1263236, 0968895, 1102301); The 863 Program (2013AA014402). Project of the Spanish Ministerio de Economía y Competitividad No. MTM2015-63914-P.

REFERENCES

1. J. C. Neu, Physica D **43**, 385 (1990).
2. A. S. Desyatnikov, L. Torner, and Y. S. Kivshar, Progress in Optics **47**, North-Holland, Amsterdam, 291 (2005).
3. G. A. Swartzlander and C. T. Law, Phys. Rev. Lett. **69**, 2503 (1992).
4. V. Tikhonenko and N.N. Akhmediev, Opt. Commun. **126**, 108 (1996).
5. A. H. Carlsson, J. N. Malmberg, D. Anderson, M. Lisak, E. A. Ostrovskaya, T. J. Alexander, and Y. S. Kivshar, Opt. Lett. **25,** 660 (2000).
6. Y. S. Kivshar and B. Luther-Davies, Phys. Rep. **298**, 81 (1998).
7. D. L. Andrews, *Structured light and its applications: An introduction to phase-structured beams and nanoscale optical forces*, in Academic Press-Elsevier (ed.), Burlington (2008).
8. S. K. Adhikari, Phys. Rev. E **92**, 042926 (2015).
9. J. R. Salgueiro, A. H. Carlsson, E. Ostrovskaya, and Y. Kivshar, Opt. Lett. **29**, 593 (2004).
10. Y. S. Kivshar, J. Christou, V. Tikhonenko, B. Luther-Davies, and L. M. Pismen, Opt. Commun. **152**, 198 (1998).
11. I. Velchev, A. Dreischuh, D. Neshev, and S. Dinev, Opt. Commun. **130**, 385 (1996).
12. D. Rozas and G. A. Swartzlander, Opt. Lett **25**, 126-128 (2000).
13. D. Rozas, C. T. Law, and G. A. Swartzlander, J. Opt. Soc. Am. B 14, 3054 (1997).
14. D. Neshev, A. Dreischuh, M. Assa, and S. Dinev, Opt. Commun. **151**, 413 (1998).
15. C. Huang, F. Ye, B. A. Malomed, Y. V. Kartashov, and X. Chen, Opt. Lett. **38**, 2177 (2013).
16. J. Zeng and B. A. Malomed, Phys. Rev. E **95**, 052214 (2017).
17. A. S. Reyna and C. B. de Araújo, Opt. Lett. **41,** 191 (2016).
18. P. Johannisson, D. Anderson, M. Lisak, and M. Marklund, Opt. Commun. **222**, 107 (2003).
19. M. A. Porras, A. Parola, D. Faccio, A. Dubietis, and P. Di Trapani, Phys. Rev. Lett. **93**, 153902 (2004).
20. P. Polesana, A. Couairon, D. Faccio, A. Parola, M. A. Porras, A. Dubietis, A. Piskarskas, and P. Di Trapani, Phys. Rev. Lett **99**, 223902 (2007).
21. M. A. Porras and C. Ruiz-Jiménez, J. Opt. Soc. Am B **31,** 2657 (2014).
22. C. Ruiz-Jiménez, PhD Thesis, DOI 10.20868/UPM.thesis.43715 (2016).
23. P. Polesana, A. Dubietis, M. A. Porras, E. Kucinskas, D. Faccio, A. Couairon, and P. Di Trapani, Phys. Rev. E **73**, 056612 (2006).
24. M. A. Porras, Márcio Carvalho, Hervé Leblond, and Boris A. Malomed, Phys. Rev. A **94**, 053810 (2016).

Informational 5th page.

REFERENCES

1. J. C. Neu, "Vortices in complex scalar fields," Physica D **43**, 385-406 (1990).
2. A. S. Desyatnikov, L. Torner, and Y. S. Kivshar, "Optical vortices and vortex solitons," in E. Wolf (ed.), Progress in Optics **47**, North-Holland, Amsterdam, 291-391 (2005).
3. G. A. Swartzlander and C. T. Law "Optical vortex solitons observed in Kerr nonlinear media," Phys. Rev. Lett. **69**, 2503-2506 (1992).
4. V. Tikhonenko and N.N. Akhmediev, "Excitation of vortex solitons in a Gaussian beam configuration," Opt. Commun. **126**, 108-112 (1996).
5. A. H. Carlsson, J. N. Malmberg, D. Anderson, M. Lisak, E. A. Ostrovskaya, T. J. Alexander, and Y. S. Kivshar, "Linear and nonlinear waveguides induced by optical vortex solitons," Opt. Lett. **25**, 660-662 (2000).
6. Y. S. Kivshar and B. Luther-Davies, "Dark optical solitons: physics and applications," Phys. Rep. **298**, 81-197 (1998).
7. D. L. Andrews, *Structured light and its applications: An introduction to phase-structured beams and nanoscale optical forces,* in Academic Press-Elsevier (ed.), Burlington (2008).
8. S. K. Adhikari, "Stable spatial and spatiotemporal optical soliton in the core of an optical vortex," Phys. Rev. E **92**, 042926 (2015).
9. J. R. Salgueiro, A. H. Carlsson, E. Ostrovskaya, and Y. Kivshar, "Second-harmonic generation in vortex-induced waveguides," Opt. Lett. **29**, 593-595 (2004).
10. Y. S. Kivshar, J. Christou, V. Tikhonenko, B. Luther-Davies, and L. M. Pismen, "Dynamics of optical vortex solitons," Opt. Commun. **152**, 198-206 (1998).
11. I. Velchev, A. Dreischuh, D. Neshev, and S. Dinev, "Interactions of optical vortex solitons superimposed on different background beams", Opt. Commun. **130**, 385-392 (1996).
12. D. Rozas and G. A. Swartzlander, "Observed rotational enhancement of nonlinear optical vortices," Opt. Lett **25**, 126-128 (2000).
13. D. Rozas, C. T. Law, and G. A. Swartzlander, "Propagation dynamics of optical vortices," J. Opt. Soc. Am. B 14, 3054-3065 (1997).
14. D. Neshev, A. Dreischuh, M. Assa, and S. Dinev, "Motion control of ensembles of ordered optical vortices generated on finite extent background," Opt. Commun. **151**, 413-421 (1998).
15. C. Huang, F. Ye, B. A. Malomed, Y. V. Kartashov, and X. Chen, "Solitary vortices supported by localized parametric gain," Opt. Lett. **38**, 2177-2180 (2013).
16. J. Zeng and B. A. Malomed, "Localized dark solitons and vortices in defocusing media with spatially inhomogeneous nonlinearity," Phys. Rev. E **95**, 052214 (2017).
17. A. S. Reyna and C. B. de Araújo, "Guiding and confinement of light induced by optical vortex solitons in a cubic-quintic medium," Opt. Lett. **41,** 191-194 (2016).
18. P. Johannisson, D. Anderson, M. Lisak, and M. Marklund, "Nonlinear bessel beams," Opt. Commun. **222**, 107-115 (2003).
19. M. A. Porras, A. Parola, D. Faccio, A. Dubietis, and P. Di Trapani, "Nonlinear Unbalanced Bessel Beams: Stationary Conical Waves Supported by Nonlinear Losses," Phys. Rev. Lett. **93**, 153902 (2004).
20. P. Polesana, A. Couairon, D. Faccio, A. Parola, M. A. Porras, A. Dubietis, A. Piskarskas, and P. Di Trapani, "Observation of Conical Waves in Focusing, Dispersive, and Dissipative Kerr Media," Phys. Rev. Lett **99**, 223902 (2007).
21. M. A. Porras and C. Ruiz-Jiménez, "Nondiffracting and nonattenuating vortex light beams in media with nonlinear absorption of orbital angular momentum," J. Opt. Soc. Am B **31,** 2657-2664 (2014).
22. C. Ruiz-Jiménez, *Dinámica no lineal de haces ópticos de Airy y de Bessel en medios Kerr con absorción no lineal,* PhD Thesis, DOI 10.20868/UPM.thesis.43715 (2016).
23. P. Polesana, A. Dubietis, M. A. Porras, E. Kucinskas, D. Faccio, A. Couairon, and P. Di Trapani, "Near-field dynamics of ultrashort pulsed Bessel beams in media with Kerr nonlinearity," Phys. Rev. E **73**, 056612 (2006).
24. M. A. Porras, Márcio Carvalho, Hervé Leblond, and Boris A. Malomed, "Stabilization of vortex beams in Kerr media by nonlinear absorption," Phys. Rev. A **94**, 053810 (2016).